

Heterogeneous Catalysis

Selective Hydrogenation of α,β -Unsaturated Aldehydes Catalyzed by Amine-Capped Platinum-Cobalt Nanocrystals**

Binghui Wu, Huaqi Huang, Jing Yang, Nanfeng Zheng,* and Gang Fu*

Nanoparticle-based metal catalysts, particularly those that have well-defined size/shape, have attracted increasing research attention for catalytic applications.^[1–4] By means of colloidal chemistry, monodisperse nanoparticles with controlled size, morphology, and composition can be synthesized through the use of stabilizing ligands.^[5–11] These shell ligands were formerly considered to hinder the catalytic/electrocatalytic activity, and were typically removed (for example, by calcination, ligand exchange, UV-ozone treatment) to evaluate the size/shape effect or metal-support interaction in catalysis/electrocatalysis.^[6–11] However, it should be noted that many studies have demonstrated that capping ligands on the surface of nanoparticles can effectively steer the chemoselectivity and enantioselectivity of nanoparticle-catalyzed liquid-phase reactions.^[12–15] For instance, self-assembled monolayer coatings of *n*-alkane thiols improve the selectivity of 1-epoxybutane formation from 1-epoxy-3-butene on Pd nanocatalysts from 11% to 94% under equivalent reaction conditions and with equivalent conversions.^[16] Enantioselective allylic alkylation reactions were achieved with 97% *ee* by using Pd nanoparticles stabilized by a chiral xylofuranoside diphosphate.^[17]

In this study, the chemoselective hydrogenation of α,β -unsaturated aldehydes (that is, cinnamaldehyde (CAL) and citral) was chosen as the model reaction for studies on the effect of capping ligands on the selectivity of nanocrystal catalysts. As the formation of the saturated aldehydes is favored over the unsaturated alcohol because of thermodynamics,^[18] the chemoselective hydrogenation of α,β -unsaturated aldehydes to the corresponding unsaturated alcohols is a scientific challenge.^[19–26] Significant efforts have been made to search for catalytic systems that are able to efficiently and selectively hydrogenate a C=O bond that is conjugated with a C=C bond.^[23,26–30] Among these, Pt nanoparticles modified with Fe, Sn, or Co were demonstrated as effective catalysts

and achieve high selectivity because of electronic and structural effects.^[26,28,29,31–36] In contrast, the effect of the surface ligands on the catalytic selectivity is less well-studied and is usually ignored. Herein, we demonstrate how the amine capping layer of Pt₃Co nanocatalysts influences the chemoselective hydrogenation of α,β -unsaturated aldehydes. Our studies reveal that amines that have longer chain lengths offer enhanced hydrogenation selectivity to α,β -unsaturated alcohols and also stability against over-hydrogenation. A steric effect from the long-chain amine is proposed to explain the enhanced selectivity.

Monodisperse, alkylamine-capped Pt₃Co alloy nanocrystals were prepared by using carbon monoxide as reducing agent according to a modified method that was described previously (see the Experimental Section and the Supporting Information for details).^[37] As detected by energy-dispersive X-ray spectroscopy (EDX) and inductively coupled plasma mass spectrometry (ICP-MS), the Pt/Co ratio in the as-synthesized nanoparticles was approximately 3:1. As shown in the typical TEM images (Figure 1; see also Figure S1 in the Supporting Information), the as-synthesized oleylamine (OAm)-capped Pt₃Co nanoparticles were uniform in size and nearly all have a truncated octahedral shape (Figure S2 in

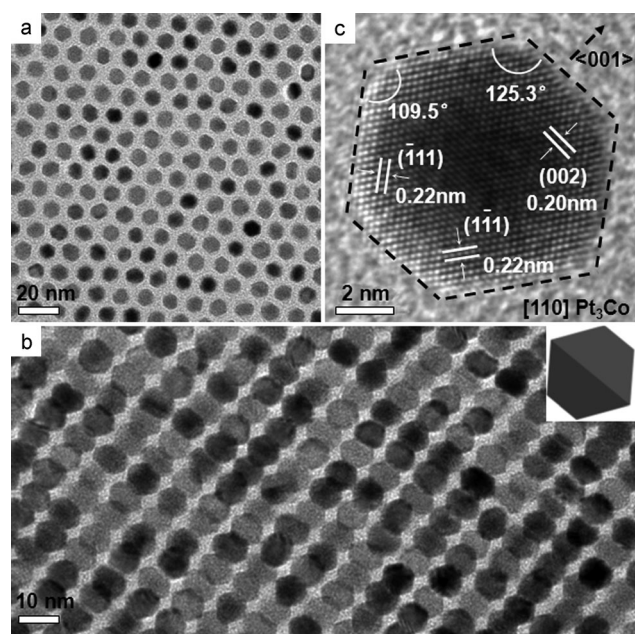


Figure 1. TEM images of 8.2 nm Pt₃Co nanoparticles. a) A monolayer assembly. b) A multilayer assembly. c) HRTEM image of a single Pt₃Co nanoparticle along the [110] zone axis. Inset in (b) is a model of truncated octahedron along the [110] zone axis with two vertices in the <001> direction cutting off from the octahedron.

[*] B. H. Wu, H. Q. Huang, Dr. J. Yang, Prof. N. F. Zheng, Prof. G. Fu State Key Laboratory for Physical Chemistry of Solid Surfaces and Department of Chemistry, College of Chemistry and Chemical Engineering, Xiamen University, Xiamen 361005 (China)
E-mail: nfzheng@xmu.edu.cn
gfu@xmu.edu.cn
Homepage: <http://chem.xmu.edu.cn/person/nfzheng/index.html>

[**] We thank the MOST of China (2011CB932403, 2009CB930703), the NSFC (21131005, 21133004, 21021061, 20925103, 20973139), the Fok Ying Tung Education Foundation (121011), the NSF of Fujian Province (Distinguished Young Investigator Grant 2009J06005), and the Fundamental Research Funds for the Central Universities for financial support.

Supporting information for this article is available on the WWW under <http://dx.doi.org/10.1002/anie.201108593>.

the Supporting Information). The average distance between the two opposite faces of the as-prepared nanoparticles was 8.2 nm. The single-crystal nature of the nanoparticles was clearly revealed by the well-resolved lattice fringes in the high-resolution TEM (HRTEM) images (Figure 1c). The average crystalline size that was estimated from Scherrer's formula by using the X-ray diffraction (111) peak (Figure S3) was approximately 8 nm, which is consistent with the dimensions shown in the TEM images.

The use of an amine as the capping agent is important to obtain the monodisperse Pt₃Co nanocrystals and to stabilize the particles against aggregation. Even after three careful purification cycles, the amine capping makes the Pt₃Co still highly dispersible in nonpolar solvents. Based on a simple truncated octahedral model, an 8 nm Pt₃Co particle has approximately 3000 metal atoms on its surface. According to the data from CNH elemental analysis and thermogravimetric analysis,^[38–39] the number of OAm molecules that are coated on each Pt₃Co nanoparticle is approximately 490. Therefore, the coverage of amine molecules on the Pt₃Co particles is estimated to be approximately 16%. By using density functional calculation (DFT) calculations (see the Supporting Information for computational details), we found that OAm can form an ordered $2\sqrt{2} \times 2\sqrt{2}$ “array” on the Pt surfaces at $\theta = 0.125$ (Figure S4 in the Supporting Information). Two possible adsorption modes have been considered, and the differences between them are the conformation of OAm, as well as the tilt angle α (Figure S5 in the Supporting Information). Although the eclipsed conformation of OAm is less stable than the staggered conformation in the gas phase, our calculations reveal that on the Pt surface, the eclipsed conformation is favored over the staggered conformation by 0.3–0.4 eV/OAm (see Table S1 in the Supporting Information). This is reasonable because the eclipsed conformation benefits more from the van der Waals interactions among the adsorbates. In this case, the long carbon chains that are capped onto the Pt₃Co nanocatalysts impart steric hindrance so that CAL molecules do not lie flat on the nanoparticle surface. Computationally, we found that CAL molecules can only enter into the array of OAm molecules edge on with their aldehyde groups interacting with the Pt₃Co (100) surface and the C=C bonds directed away from the catalytically active surface (Figure 2a). The predicted adsorption energy is -0.63 eV relative to the OAm-capped surface, and the C=O bond is elongated to 1.370 Å, which indicates that the C=O bonds in CAL molecules can be hydrogenated more easily than the C=C bond. To demonstrate such chemoselectivity, we carried out the hydrogenation under H₂ (1.5 atm) at 25 °C catalyzed by 8.2 nm OAm-capped Pt₃Co nanoparticles. The conditions were much milder than many previous reports, in which high temperature (80 °C or more) and high pressure (for example, 20 bars) were used.^[28,29] As illustrated in Figure 2b, our OAm capped Pt₃Co nanoparticles catalyzed the hydrogenation of CAL. Within 9 h, the hydrogenation of CAL was completed with a selectivity for the cinnamyl alcohol (COL) of up to 95%. The selectivity for the undesired saturated aldehyde hydrocinnamaldehyde (HCAL) and the saturated alcohol hydrocinnamyl alcohol (HCOL) remained low, which supports our theoretical prediction.

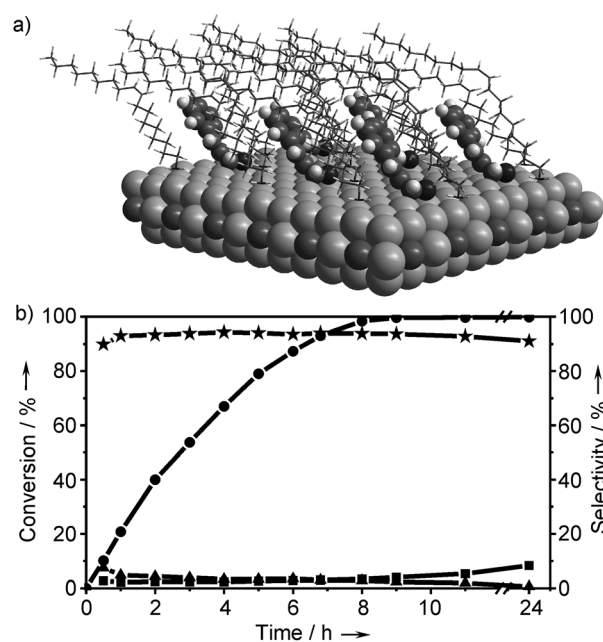


Figure 2. a) Optimized structure of CAL adsorption (ball-and-stick) on the Pt₃Co(100) surface capped by OAm (line). Key bond distances: $R_{C-O} = 1.370$ Å; $R_{C-C} = 1.356$ Å. b) Curves of conversion of CAL (●) and selectivity for COL (★), HCAL (▲), and HCOL (■) from the hydrogenation of CAL with OAm-capped Pt₃Co nanocatalysts. Conditions: Pt₃Co nanocatalysts (11 mg), *n*-butanol (10 mL), CAL (3 mmol), nonane (1 mmol), H₂ (1.5 atm), 25 °C.

What was even more surprising was that the selectivity for COL was not reduced much by lengthening the reaction time. When the reaction time was extended to 24 h, the selectivity for COL was still above 90%. In contrast, the small amount of HCAL that was produced was converted to HCOL by further reduction of the carbonyl group. These results suggest that the hydrogenation of C=C and C=O bonds does not take place in parallel on the OAm-capped Pt₃Co nanoparticles, which is different from previous reports.^[27,33] Being able to prevent the C=C bonds of COL from further hydrogenation over a long period suggests that the steric effect that is created by the surface OAm molecules cannot be easily destroyed under the reaction conditions. Even when high temperature (80 °C) and high H₂ pressure (4 atm) was applied to the reactions (Figure S6 in the Supporting Information), the selectivity for COL was over 95%, which confirms that the steric effect created by the OAm molecules on the surface is fairly stable.

It should be noted that the steric effect of OAm on the catalytic selectivity was also effective in the hydrogenation of other α,β -unsaturated aldehydes. For example, as a natural product, citral is a mixture of two isomeric forms: 50% neral (*cis*-form) and 50% geranial (*trans*-form, Figure 3). When OAm-capped Pt₃Co nanoparticles were applied as the catalysts under the mild reaction conditions, the C=O bonds of both isomeric forms were easily hydrogenated with a selectivity of above 90%. However, the OAm-capped Pt₃Co particles were more active in the hydrogenation of geranial than neral, which can be explained by a larger steric hindrance for neral in the OAm capping layer. The results from the hydrogenation of citral reinforce our hypothesis on the steric effect of the amine capping agents on the catalytic

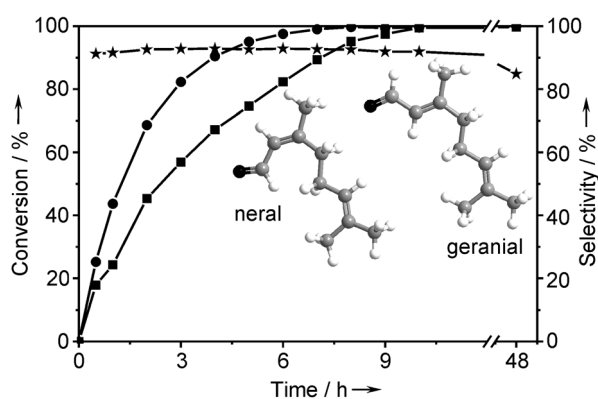


Figure 3. Curves of conversion of neral (■) and geranial (●) and total C=O selectivity (★) for products from the hydrogenation of citral with OAm-capped Pt₃Co nanocatalysts. Conditions: Pt₃Co nanocatalysts (11 mg), *n*-butanol (10 mL), citral (3 mmol, 1:1 neral and geranial), nonane (1 mmol), H₂ (1.5 atm), 25 °C.

performance of OAm-capped Pt₃Co nanoparticles (Figure 2a).

OAm can help to prevent CAL from lying flat on the metal surface, which leads to high selectivity towards COL. Now the question emerges as to how CAL interacts with the catalytically active sites when a shorter-chain amine is used. In this case, a C₄NH₂/Pt₃Co system was used as an instructive case. DFT (PBE/PAW) calculations demonstrate that the adsorption energies for C₄NH₂ onto different Pt₃Co surfaces are nearly equal to those for OAm (see Table S1 in the Supporting Information). However, when dispersion interactions are taken into account, that is, DFT-D, C₄NH₂ becomes 0.3–1.0 eV per amine molecule less favorable than OAm, as the latter has a longer carbon chain. This indicates that, unlike OAm, C₄NH₂ is liable to diffuse on the surface or to be liberated into the solvent, which might, in turn, destroy the ordered “array”. We also estimated the rotation barriers of both OAm and C₄NH₂ around the C–N bond on the Pt₃Co (100) surface (Figure S7 in the Supporting Information). Interestingly, we found that converting from the eclipsed conformation into the staggered conformation that is, increasing ϕ from approximately 80° to 160°, has to overcome a barrier of 1.4 eV per amine molecule, which means that the conformation of the OAm array is rather rigid once formed. In contrast, the conformation of C₄NH₂ on the surface is rather fluxional, as the predicted barrier for such a rotation is only approximately 0.1 eV per amine molecule. All these results indicate that when shorter-chain amines are used as capping agents, the α,β -unsaturated aldehyde are still able to lie flat on the surface of the metal. Indeed, we did locate a structure in which CAL can adsorb onto C₄NH₂/Pt₃Co (100) at $\theta = 0.125$ through the C=C bond of CAL (Figure S8 in the Supporting Information). In this case, the C=C bond is significantly activated ($R_{C-C} = 1.444 \text{ \AA}$), and the calculated adsorption energy is -1.30 eV . To prove this experimentally, Pt₃Co nanocrystals with a similar size, shape, and composition but capped by various amines (C₁₈NH₂, C₁₆NH₂, C₁₂NH₂) were synthesized under conditions similar to OAm-capped Pt₃Co nanoparticles, or by ligand exchange with OAm-capped nanoparticles with the target amines (C₈NH₂ or C₄NH₂;

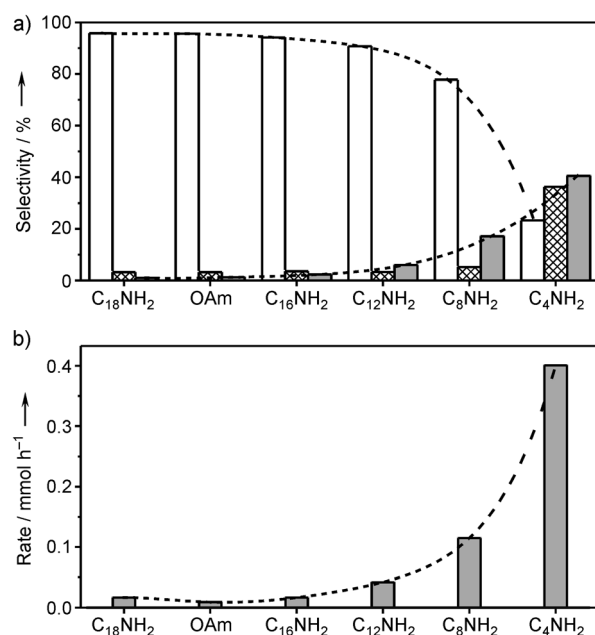


Figure 4. Histograms of a) Selectivity for COL (white), HCAL (cross-hatch), and HCOL (gray) at nearly 100% conversion in the hydrogenation of CAL with different amine-capped Pt₃Co catalysts. b) Rates of HCOL production after complete conversion of CAL with different amine-capped Pt₃Co nanocatalysts. Conditions: Pt₃Co nanocatalysts (11 mg), *n*-butanol (10 mL), CAL (3 mmol), nonane (1 mmol), H₂ (1.5 atm), 25 °C.

Figure S9 in the Supporting Information; see also the Supporting Information for details of the synthesis).

Figure 4a shows the ligand-dependent selectivity in the catalytic hydrogenation of CAL. The results reveal that the selectivity for COL gradually decreases with the shortening of the chain length of the amines that are coated onto the Pt₃Co nanocrystals. The Pt₃Co nanocatalysts that are coated with C₁₈NH₂, OAm, C₁₆NH₂, and C₁₂NH₂ catalyzed the hydrogenation with a high selectivity of over 90% for COL at 100% conversion of CAL. In comparison, the Pt₃Co particles that are capped by C₈NH₂ gave a medium selectivity for COL at approximately 78%. The C₄NH₂-capped nanocatalysts led to the lowest selectivity at approximately 23% at 100% conversion of CAL. The relatively low selectivity for COL by C₄NH₂-capped nanoparticles implies that both C=O and C=C bonds can competitively access the metal surface during the reaction. When shorter-chain amines (that is, C₈NH₂ or C₄NH₂) were used as the capping ligands, the catalysts easily hydrogenated COL further into HCOL over time (Figure 4b; see also Figures S10 and S11 in the Supporting Information). The shorter the chain, the higher the yield of over-hydrogenated products. Whereas the shorter chain length of the capping amines is deleterious to the selectivity for COL, it is beneficial to the diffusion of CAL molecules onto the catalytic metal surface and, thus, enhances the hydrogenation activity. Indeed, our studies reveal that the catalytic activity by Pt₃Co nanoparticles capped by different amines is highly dependent on the chain length of the capping amines (Figure S12 in the Supporting Information). A shorter-chain capping amine offers higher activity in the hydrogenation.

In summary, we have demonstrated that amine-capped Pt₃Co-alloy nanoparticles can be used as efficient catalysts for the selective hydrogenation of α,β -unsaturated aldehydes under mild conditions. Detailed studies and periodic DFT calculations reveal that the presence of long-chain amines on the surface of the nanoparticles is essential for the high selectivity of the hydrogenation towards α,β -unsaturated alcohols. A steric effect in long-chain amines prevents α,β -unsaturated aldehydes lying flat on the surface and, therefore, avoids direct contact of the C=C bonds with the catalytic Pt₃Co surface. Longer carbon chains give higher selectivity. This study provides an important insight into how organic capping layers control the catalytic performance of metal nanocrystals.

Experimental Section

8.2 nm OAm-capped Pt₃Co nanocatalysts were synthesized as follows: [Pt(acac)₃] (20 mg) and [Co(acac)₃] (10 mg) were dissolved in OAm (10 mL) in a flask that was immersed in a water bath at 50 °C, and stirred for 10 min (simultaneously a CO flow was applied into the flask to remove air). The outside of the flask was dried and the flask was directly immersed into an oil bath that was preheated to 240 °C. The mixture was kept stirring at 240 °C with a CO flow (ca. 50 mL min⁻¹) for 40 min. The black dispersion was then cooled to room temperature, precipitated out with ethanol, and washed twice with cyclohexane/ethanol. Other amine-capped Pt₃Co nanoparticles were synthesized by ligand exchange, or under the same conditions described above, but changing the type of amine.

Catalytic hydrogenation of CAL was carried out in a well-stirred glass pressure vessel (48 mL) at room temperature. The Pt₃Co nanocatalysts were dispersed in butanol (5 mL) by ultrasound, and then transferred into the pressure vessel. A mixture of butanol (5 mL), nonane (1 mmol, used as an internal standard), and CAL (3 mmol) was added. H₂ flow was applied into the vessel for several minutes to remove any traces of oxygen. The vessel was pressurized with H₂ (1.5 atm). The reaction was then allowed to proceed and samples were withdrawn at regular intervals, filtered, and analyzed by gas chromatography (GC) and gas chromatography-mass spectrometry (GC-MS).

Received: December 5, 2011

Published online: February 28, 2012

Keywords: aldehydes · alkenes · hydrogenation · ligand effects · nanoparticles

- [1] T. S. Ahmadi, Z. L. Wang, T. C. Green, A. Henglein, M. A. El-Sayed, *Science* **1996**, 272, 1924–1926.
- [2] G. A. Somorjai, A. M. Contreras, M. Montano, R. M. Rioux, *Proc. Natl. Acad. Sci. USA* **2006**, 103, 10577–10583.
- [3] Y. Li, Q. Liu, W. Shen, *Dalton Trans.* **2011**, 40, 5811–5826.
- [4] D. W. Goodman, *Surf. Sci.* **1994**, 299–300, 837–848.
- [5] K. M. Bratlie, H. Lee, K. Komvopoulos, P. D. Yang, G. A. Somorjai, *Nano Lett.* **2007**, 7, 3097–3101.
- [6] M. Comotti, W. C. Li, B. Spliethoff, F. Schuth, *J. Am. Chem. Soc.* **2006**, 128, 917–924.
- [7] N. F. Zheng, G. D. Stucky, *J. Am. Chem. Soc.* **2006**, 128, 14278–14280.
- [8] C. Aliaga, J. Y. Park, Y. Yamada, H. S. Lee, C. K. Tsung, P. D. Yang, G. A. Somorjai, *J. Phys. Chem. C* **2009**, 113, 6150–6155.

- [9] J. B. Wu, J. L. Zhang, Z. M. Peng, S. C. Yang, F. T. Wagner, H. Yang, *J. Am. Chem. Soc.* **2010**, 132, 4984–4985.
- [10] J. Zhang, H. Z. Yang, J. Y. Fang, S. Z. Zou, *Nano Lett.* **2010**, 10, 638–644.
- [11] C. Wang, H. Daimon, T. Onodera, T. Koda, S. H. Sun, *Angew. Chem.* **2008**, 120, 3644–3647; *Angew. Chem. Int. Ed.* **2008**, 47, 3588–3591.
- [12] D. Astruc, F. Lu, J. R. Aranzas, *Angew. Chem.* **2005**, 117, 8062–8083; *Angew. Chem. Int. Ed.* **2005**, 44, 7852–7872.
- [13] M. Heitbaum, F. Glorius, I. Escher, *Angew. Chem.* **2006**, 118, 4850–4881; *Angew. Chem. Int. Ed.* **2006**, 45, 4732–4762.
- [14] T. Mallat, E. Orglmeister, A. Baiker, *Chem. Rev.* **2007**, 107, 4863–4890.
- [15] F. Zaera, *Acc. Chem. Res.* **2009**, 42, 1152–1160.
- [16] S. T. Marshall, M. O'Brien, B. Oetter, A. Corpuz, R. M. Richards, D. K. Schwartz, J. W. Medlin, *Nat. Mater.* **2010**, 9, 853–858.
- [17] S. Jansat, M. Gomez, K. Philippot, G. Muller, E. Guiu, C. Claver, S. Castillon, B. Chaudret, *J. Am. Chem. Soc.* **2004**, 126, 1592–1593.
- [18] P. Mäki-Arvela, J. Hajek, T. Salmi, D. Y. Murzin, *Appl. Catal. A* **2005**, 292, 1–49.
- [19] P. Gallezot, B. Blanc, D. Barthomeuf, M. I. Païs da Silva, *Stud. Surf. Sci. Catal.* **1994**, 84, 1433–1439.
- [20] E. J. Creighton, R. S. Downing, *J. Mol. Catal. A* **1998**, 134, 47–61.
- [21] C. Mohr, N. Hofmeister, M. Lucas, P. Claus, *Chem. Eng. Technol.* **2000**, 23, 324–328.
- [22] A. Solhy, B. F. Machado, J. Beausoleil, Y. Kihn, F. Goncalves, M. F. R. Pereira, J. J. M. Orfao, J. L. Figueiredo, J. L. Faria, P. Serp, *Carbon* **2008**, 46, 1194–1207.
- [23] L. He, F. J. Yu, X. B. Lou, Y. Cao, H. Y. He, K. N. Fan, *Chem. Commun.* **2010**, 46, 1553–1555.
- [24] Y. Zhu, H. F. Qian, B. A. Drake, R. C. Jin, *Angew. Chem.* **2010**, 122, 1317–1320; *Angew. Chem. Int. Ed.* **2010**, 49, 1295–1298.
- [25] R. E. Eilerman, J. I. Kroschwitz, *Kirk-Othmer Encyclopedia of Chemical Technology*, Wiley, New York, **1992**.
- [26] A. B. Merlo, B. F. Machado, V. Vetere, J. L. Faria, M. L. Casella, *Appl. Catal. A* **2010**, 383, 43–49.
- [27] J. P. Breen, R. Burch, J. Gomez-Lopez, K. Griffin, M. Hayes, *Appl. Catal. A* **2004**, 268, 267–274.
- [28] Y. Li, Z. G. Li, R. X. Zhou, *J. Mol. Catal. A* **2008**, 279, 140–146.
- [29] S. C. Tsang, N. Cailuo, W. Oduro, A. T. S. Kong, L. Clifton, K. M. K. Yu, B. Thiebaut, J. Cookson, P. Bishop, *Acs Nano* **2008**, 2, 2547–2553.
- [30] Y. C. Hong, K. Q. Sun, G. R. Zhang, R. Y. Zhong, Q. Xu, *Chem. Commun.* **2011**, 47, 1300–1302.
- [31] V. Brotons, B. Coq, J. M. Planeix, *J. Mol. Catal. A* **1997**, 116, 397–403.
- [32] P. Gallezot, D. Richard, *Catal. Rev. Sci. Eng.* **1998**, 40, 81–126.
- [33] W. Y. Yu, H. F. Liu, M. H. Liu, Q. Tao, *J. Mol. Catal. A* **1999**, 138, 273–286.
- [34] B. J. Liu, G. X. Xiong, X. L. Pan, S. S. Sheng, W. S. Yang, *Chin. J. Catal.* **2002**, 23, 481–484.
- [35] X. X. Han, R. X. Zhou, X. M. Zheng, *Indian J. Sci. Ind. Sect. A* **2006**, 45, 1646–1650.
- [36] Y. Li, R. X. Zhou, G. H. Lai, *React. Kinet. Catal. Lett.* **2006**, 88, 105–110.
- [37] B. H. Wu, N. F. Zheng, G. Fu, *Chem. Commun.* **2011**, 47, 1039–1041.
- [38] M. Shen, Y. K. Du, N. P. Hua, P. Yang, *Powder Technol.* **2006**, 162, 64–72.
- [39] M. Moreno, F. J. Ibanez, J. B. Jasinski, F. P. Zamborini, *J. Am. Chem. Soc.* **2011**, 133, 4389–4397.